Strategies for conformal REBCO windings

J S Rogers[1], P M McIntyre[1,2], T Elliott[2], G D May[1] and C T Ratcliff[1]

[1]Texas A&M University

[2]Accelerator Technology Corp.

E-mail: jsr12e@tamu.edu

Abstract. A high-field winding can be fabricated from a cable of non-insulated REBCO tapes stacked face-to-face without twisting. If the cable is oriented within each turn of a winding so that the tape face is closely parallel to the magnetic field at its location, the supercurrent capacity of that cable is enhanced ~3x greater than in a transverse or twisting orientation. This concept for a conformal winding was presented in a previous paper pertinent to the body winding of a REBCO based high-field dipole. Strategies are presented and simulated for how the same orientation can be sustained in the flared ends of a high-field hybrid dipole.

1. Introduction

REBCO tape has remarkable properties for use in superconducting magnets. It can operate with useful current density up to liquid nitrogen temperature and it can produce very high magnetic field at temperatures of 20-40 K. The manufactured tape is ready to use as supplied and does not require a final heat treatment after winding into a magnet winding – an important benefit compared to Nb_3Sn and Bi-2212.

On the other hand, REBCO has undesirable properties that have limited its usefulness in high field magnets. REBCO is ruinously expensive, making it infeasible for use in many applications. Additionally, it is a highly [1]anisotropic superconductor [1] with a critical current that is strongly dependent on the magnitude and direction of the magnetic field in which it is operating (Figure 1). The critical current is approximately 3x greater when the magnetic field at the tape is parallel to the tape face ($B_{\parallel}, \theta = 90°$) than when it is perpendicular ($B_{\perp}, \theta = 0°$).

In a previous paper, a conformal winding method was presented in which a REBCO winding was configured in a dipole such that the tapes within the winding are everywhere oriented parallel to the field at the tape, enabling the winding to use the full capacity of the REBCO films. In this work we use a REBCO insert winding as the core of a hybrid dipole which as obeys this conformity with the field lines. Figure 2 shows an example field design for such a dipole. The insert winding consists of a tape-stack cable in which 25 REBCO tapes are stacked face-to-face, and each turn of the cable is oriented closely parallel to the field at that location.

*Awaiting publication in proceedings of the 2021 joint Cryogenics Engineering Conference and International Cryogenic Materials Conference (CEC/ICMC)

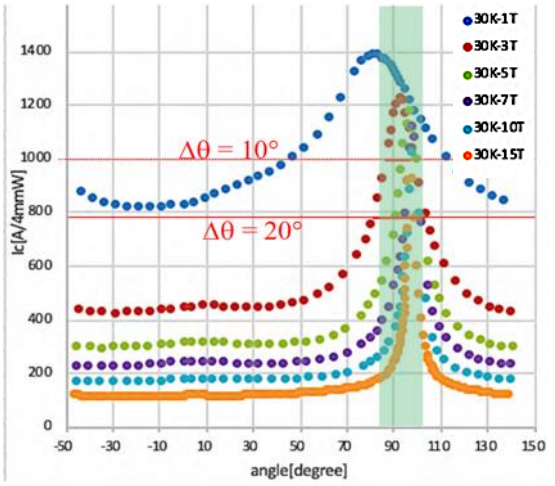

Figure 1. Dependence of I_c on the angle between the tape face normal and the magnetic field, for various field strengths (30 K temperature, from [1]).

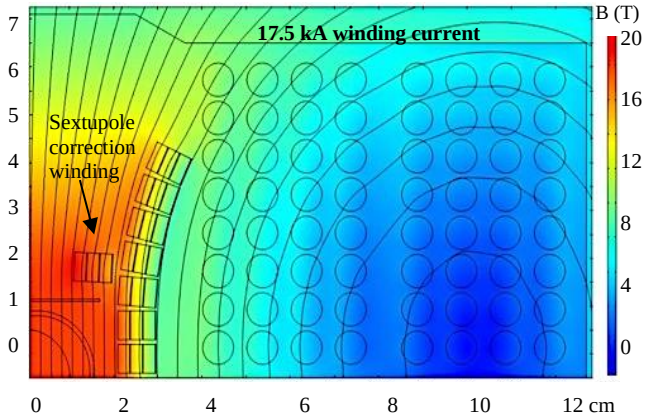

Figure 2. Field distribution in one quadrant of an 18 T dipole conformal REBCO winding. The field magnitude is shown in color while black lines show contours of the A_z component of the vector potential, ie. "lines of force"

Clustering REBCO tapes has been used by several authors including Roebel cable [2], CORC [3], cable-in-conduit [4], and stacked tapes [5]. In most cases REBCO tapes are stacked in a face-on cluster and then multiple clusters are cabled around a solid copper core with a twist pitch so that each cluster spends equal length on the inside and outside of the cable in a winding. Yagotintsev *et al*. [6] review the measurements of AC loss and contact resistance in these several forms of clustered-tape conductors. All the present approaches to tape clustering involve twisting the cluster and thus forego any possibility to sustain the $B_{\|}$ condition that would allow the REBCO tape to be used at its full potential; this is the goal of the conformal winding method.

There are two challenges in making the conformal winding realizable:

- Can uniformly high critical current be sustained in the end windings of the dipole insert (where the magnetic field and the winding must both be flared) and in the leads, as it is in the body?
- Can the tape-cluster cable support dynamic current-sharing within each cable turn so that inductive forces within the non-insulated cable do not concentrate its current in outer tapes and drive premature quench?

2. Optimization of conformal winding

The hybrid dipole shown in Figure 2 contains an insert winding made from rectangular REBCO tape-stack cable and an outsert winding made from Nb_3Sn Cable-in-Conduit 'SuperCIC' [7]. Table 1 summarizes the main parameters of both windings. The tape-stack cable contains 25 6-mm-wide REBCO tapes with 100 μm Cu clad to one side. The SuperCIC cable contains 17 0.85 mm-diameter

Table 1. Main parameters of the 18 T hybrid dipole.

Bore field @ 4.2K short-sample	18.3	T
Cable current (windings in series)	17.5	kA
Aperture: horizontal, vertical	40, 30	mm
REBCO: #tapes/cable x #cables/shell x #shells	25x 16 x 3	
Nb_3Sn CIC: #wires/CIC x #cables/layer x #layers	17x 16 x 8	
B_{max} in REBCO, CIC	20.0, 11.8	T
Sextupole @ full field, injection field	-5, -21	units

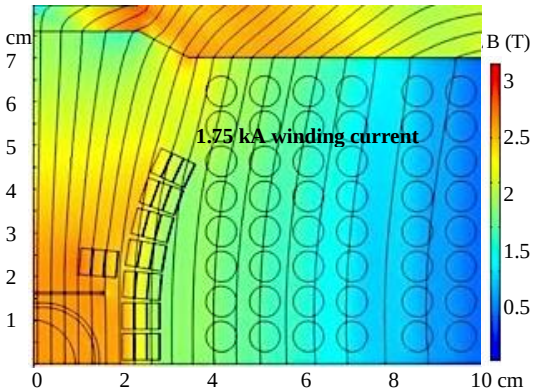

Figure 3. Field distribution at injection field.

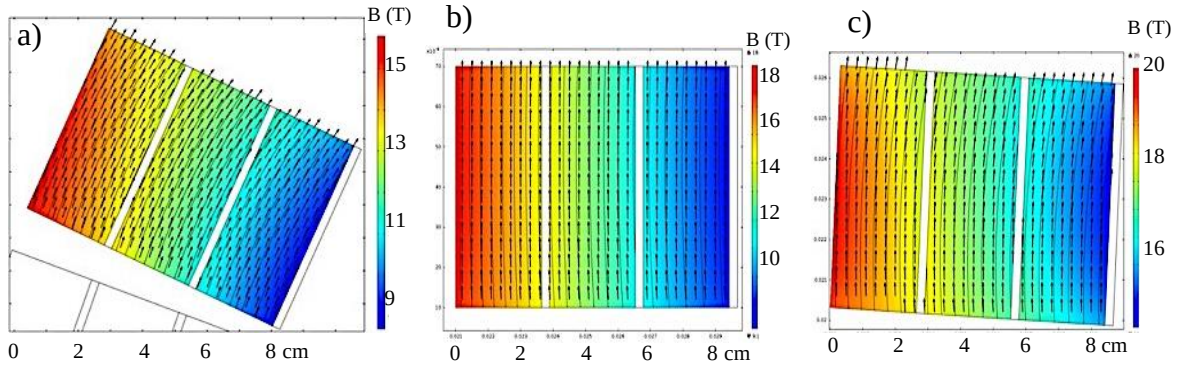

Figure 4. Detailed simulation of the fields on the tape faces for a) top right; b) mid-plane; and c) sextupole 3-turn blocks of tape-stack cables in the REBCO insert winding. Shown in color are the field magnitudes while black arrows represent the direction of the field vectors

wires of Hi-Lumi-class 108/127 Nb_3Sn/Cu wires, spiral-wrapped as a single layer around a thin-wall perforated center tube, then pulled to a loose fit through a bronze sheath tube and drawn to compress the wires against the center tube to immobilize them. The winding is housed in a steel flux-return shown as the outer rectangular boundary in Figure 2.

The windings are operated in series, and the number of wires in each winding are chosen so that a cable current of 17.5 kA produces ~18 T bore field and corresponds approximately to the critical current in each winding. The REBCO insert can operate at up to 20K, while the Nb_3Sn winding operates at ~5K.

2.1. Conformal geometry at injection field

The field distribution in the winding region is significantly different at injection field than at collision field, due to progressive saturation in the flux return. Figure 3 shows the field distribution at injection field (1.75 kA winding current). There is a significant angle θ between the tape face and the field direction in several blocks, but the value of $|B|$ is low enough that the critical current $I_c(|B|, \theta)$ is sufficient that there is no risk of quenching provided that current sharing is dynamically stable.

2.2. Body field simulations

The rectangular REBCO tape stack cables are oriented along a curving contour to conform with the flaring behavior of the magnetic field in the region of the insert winding. The cylindrical CIC cables are oriented in a rectangular block-coil array in the outsert winding. There is also a 'sextupole correction' sub-winding of REBCO cables located inside and above the main REBCO insert, which is operated in series to correct sextupole field in the bore. Immediately above the bore tube is a steel flux plate that suppresses multipoles at injection field to suppress the effects of persistent currents and snap-back at injection field. The REBCO insert contributes ~8T and the CIC winding ~10T to the bore field.

Figure 4 shows a detailed cross-section of 3 particular 3-turn blocks within the REBCO insert winding: the top-right block, the mid-plane block, and the sextupole block. These blocks exhibit variously the highest field or the maximum deviation from the $B_{\parallel}$ orientation for some of the constituent tapes. The current capacity of the *m*th tape in each cluster can be estimated by extracting the local sheet critical current density $K_m(u)$ as a function of the location u across the width of that tape, using the local values for $|B(x,y)|$ and θ, and adding the contributions for segments spanning the entire width w of that tape: $I_{cm} = \int_0^w K_m(u)du$. The total cable current capacity is then obtained by adding the maximum current capacity of the 25 tapes in that cable segment.

2.3. End field Simulations

An additional challenge is to design a winding strategy for the magnet ends that does not compromise the operational current capacity. In the 3D end regions of the dipole, fields flare and bend in a disorderly fashion raising concerns about the critical current of the cables. The flared ends of the tape-stack winding are formed using a method first pioneered by Willy Sampson (BNL) in the 1970s. Figure 5 shows a flared-end quadrupole containing a stacked-tape winding of dip-process Nb_3Sn tape. Each tape-stack

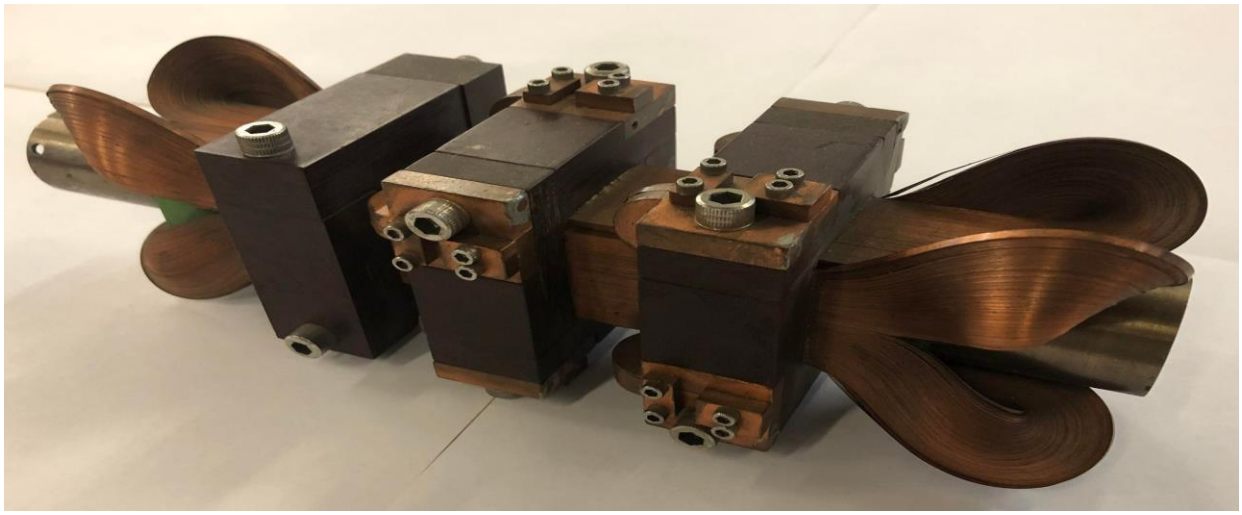

Figure 5. Example of flared ends in a tape-stack cable: Sampson's flared-end quadrupole using dip-coated Nb_3Sn superconducting tape.

cable is twisted about its axis as it is flared vertically to form a catenary. All tapes remain as a stack but no tape is bent in the hard direction. With this approach each tape face naturally follows closely the flaring of the magnetic field in the end.

This twisted-flare end has been modeled in a 3-D CAD design, and the fields have been modeled using 3-D Magnetic Field simulations in COMSOL. Figure 6 shows the results in three example cross sections through the end region: a) a y/z cross section through the vertical midplane; b) an x/y cross section at the transition from body to flared end; and c) an x/y cross section at a location 3 cm into the body from that transition. The $I_c(|B|, \theta)$ for each tape is estimated using the data of Figure 1 and then is summed across all tapes to obtain the I_c in each tape-stack cable at that location.

There is a compensating interplay that sustains I_c with little or no degradation through the flared ends: the inner tapes are well-aligned to with the field direction but have the strongest value. Although the outer tapes flare at a significant angle with respect to the field, the field strength is low enough that the angular dependence of $I_c$is also broadened. *The flared-end regions do not present a 'weak link' limit to the I_c of the cable in any turn of the winding.*

3. Dynamic current-sharing in the conformal winding

The current sharing strategy in the cable is based on the interplay of Lorentz forces acting on currents and contact resistance between stacked-tape faces during operation. Figure 7 shows a 3-turn block of cables detailing the 25 layers of stacked tape in each cable, insulation between cable turns, and a laminar spring that provides uniform compression of tape stacks. Here we employ the current sharing strategy proposed in our previous work [8] in which a conformal winding for a 3.5T dipole with only REBCO (no outsert winding) was designed**.** In summary, as the dipole is ramped to increase the bore field from its value at injection energy to that at collision energy, the total current entering each tape-cluster cable is increased. As shown in Figure 8, the magnetic field at each cable produces a Lorentz force $\vec{F}$ that redistributes the current density flowing within each tape-cluster cable away from the dipole bore. This implies that as the cable current is increased the outermost tape would quench prematurely while the current in neighboring tapes of that cable was still only a fraction of their critical current.

However, there is a countervening effect as discussed by Trillaud *et al*. [9]. As the current in each tape approaches its limit, the internal dynamics within its REBCO layer shifts from flux creep to flux flow before reaching the normal state (as demonstrated in Figure 1 from [9]). The local electric field in the tape increases exponentially with current:

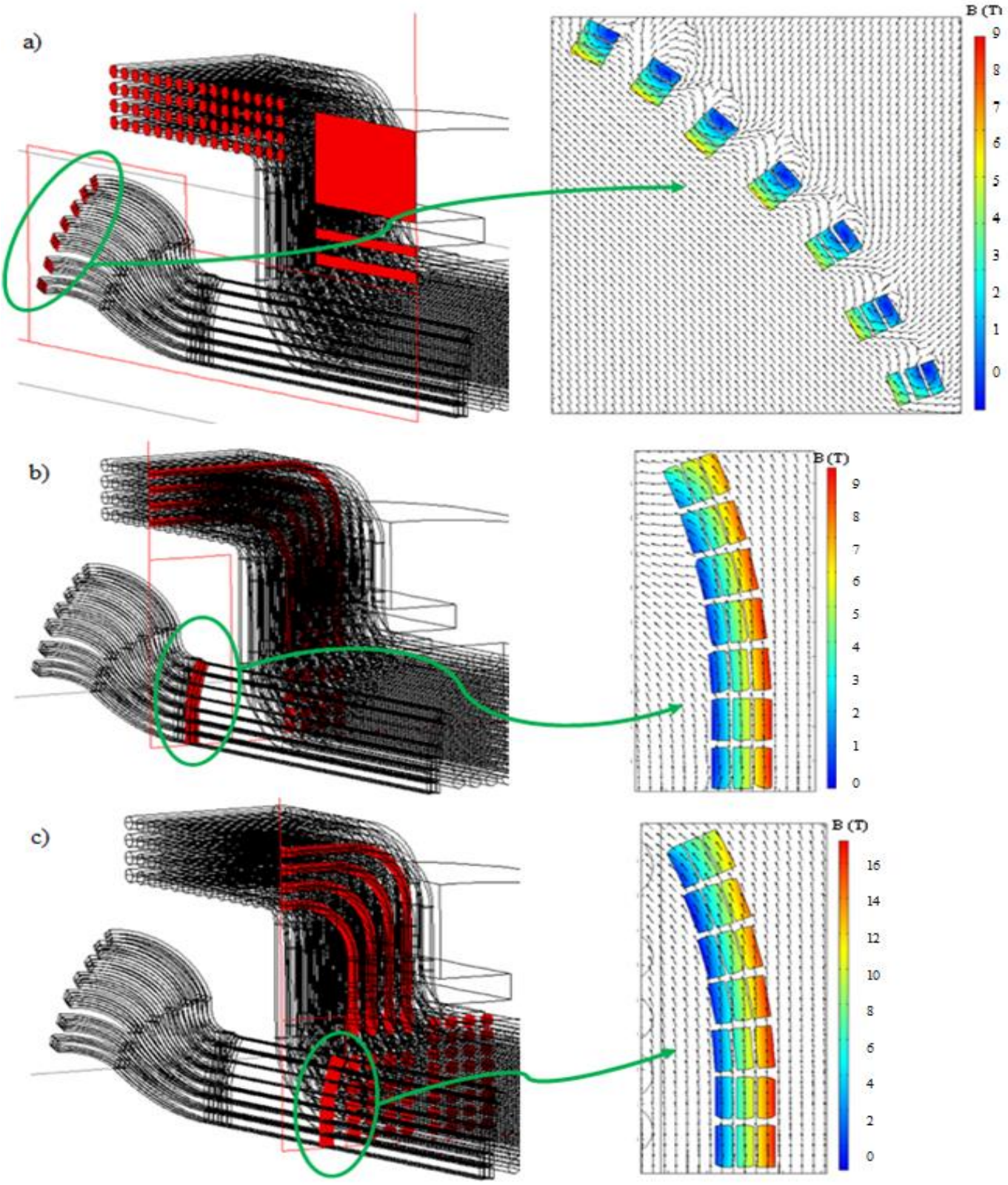

Figure 6. Three sections through the REBCO end winding of the hybrid dipole: a) section through the vertical midplane; b) x/y cross section at the transition from body to end winding; c) x/y cross-section 3 cm into the body winding. Black arrows indicate field directions.

$$E_z = E_0(I/I_c)^n \quad (1)$$

where $E_0 = 10^{-6}\frac{V}{m}$ is the quench criterion, $I_c(|B|, \theta, T)$ is the critical current for the conditions (B, θ, T)

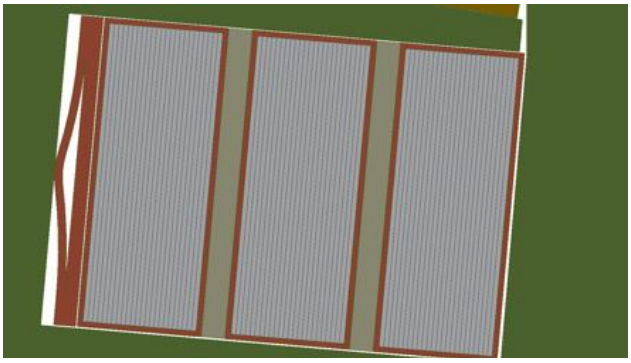

Figure 7. Detail showing a block of 3 tape-stack tapes, each containing 25 tapes, with a laminar spring to provide uniform ~1 MPa compression to all cables and insulation space between cable turns.

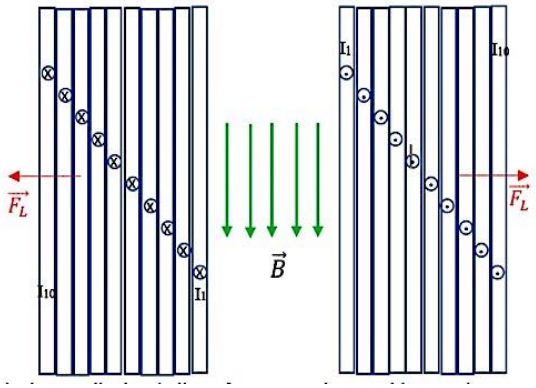

Figure 8. Schematic illustration of current-sharing dynamics in a conformal winding of tape-stack REBCO cable.

for that tape, and $n \sim 30$ is the index that characterizes the power-law dependence of the superconductor-normal transition for REBCO. As the current I in a given tape approaches I_c, the generated E_z causes the current in that tape to redistribute into the neighboring tapes where $I \ll I_c$. Since REBCO can operate at temperatures >20 K where the heat capacity of the tape ($\sim T^3$) is much greater than that in low-temperature superconductors, it is feasible to remove the generated heat so that a local 'soft-quench' in a tape segment drives re-distribution of current within the cable rather than propagating. This pattern repeats for neighboring tapes as the current is ramped.

The 'soft quench' approach has been used to good effect in 'non-insulated' (NI) pancake windings for high-field solenoids [10] but never in a dipole. The dynamics of quasi-equilibrium current sharing among the tapes within a non-transposed cable follows nearly identically to those detailed in [8]. The model uses the approach for NI REBCO pancake coils by Noguchi [11] and relies on tape face-to-face contact resistance that decreases with compression as measured by Lu *et al*. [12] shown in Figure 9.

There is interesting physics in the current-sharing among NI REBCO tapes that are face-aligned with $\vec{B}$. The above qualitative model lays the groundwork to develop a multi-scale model connecting the normal transition at nanoscale to the redistribution of currents and forces among the tapes and will be the focus of future work.

4. Field homogeneity for collider requirements

Field homogeneity is of particular concern for the dipole magnets of an accelerator or collider. The sextupole harmonic can be selectively canceled by placement of one correction turn in the winding, at the location shown in Figure 2. This magnetic design shown has been optimized to produce nearly pure dipole field over a dynamic range of field 0.2-4 T in which the amplitudes b_n are all less than 10^{-4}.

Current sharing poses a further challenge for field homogeneity. However, at injection field, the current in each tape cluster is located mainly in the outermost tape; at collision field, the current is approximately equally shared, so the 'current location' for that cable turn is shifted inwards by half the cluster width.

Conventionally, the n[th] multipole of a dipole field distribution is defined at a location $\vec{r} = r(\hat{x}cos\theta + \hat{y}sin\theta)$ by the expansion:

$$B_x + iB_y = \sum b_n e^{-ni\theta} \left(\frac{r}{R}\right)^{n-1} \qquad (2)$$

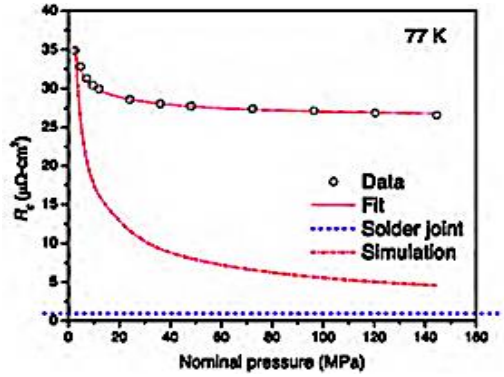

Figure 9. Contact resistance between two copper-clad REBCO tapes as a function of compression.

Here the multipole coefficients b_n are defined as,

$$b_n = \frac{1}{\pi B_0}\left(\frac{R_{ref}}{r}\right)^n \int_0^{2\pi} B_y(\theta)\cos(n\theta)\,d\theta \quad (3)$$

where R_{ref} is a reference radius that is generally taken to be ~66% of the aperture. It is convenient to take $r = R_{ref}$ and to follow the convention that $b_0 = 1$, thereby implying:

$$B_0 = \frac{1}{\pi}\int_0^{2\pi} B_y\,d\theta \quad (4)$$

The multipoles have been evaluated for the magnetic design for the maximum and injection field limiting cases. The difference in the calculated multipoles is $\Delta b_n < 0.5 \times 10^{-4}$ for all multipoles! This remarkable result is a consequence of the conformal design strategy: since each tape cluster is oriented with its face closely parallel to $\vec{B}$, the field distribution is insensitive to the horizontal position of the 'current location' of that cluster.

Prestemon *et al*. [13] modeled current transfer in a stacked-tape cable and found that a region of cable with coupling resistance $R{\sim}10\ n\Omega$ is effective in equalizing current among its tapes. The laminar spring sustains $1\ MPa$ compression giving a contact resistance $R_c{\sim}35\mu\Omega\cdot cm^2$. For a tape of width $w = 6mm$ the characteristic length of cable for stability is

$$L = \frac{R_c}{R\cdot w} \sim \frac{35\mu\Omega\cdot cm^2}{10n\Omega\cdot 6mm} = 60\text{m} \quad (5)$$

This is conveniently the approximate length for one turn of a collider dipole so ramping current should stabilize turn-by-turn.

5. Conclusion

A strategy is presented by which a cable containing multiple REBCO tapes may be configured in an insert magnet winding in such a way that the favourable $B_\parallel$ orientation is sustained everywhere in the body of the winding such that the REBCO tapes could perform to their maximum potential. An Nb_3Sn SuperCIC outsert winding shapes the fields on the tapes and adds to the total bore field. A method for dynamic current sharing is discussed, in which current would naturally re-distribute among the tapes of each cable turn as windng current is increased without inducing premature quench. Dynamics and field multipoles at different stages of operating current were studied, as well as stabililty during the ramping process.

6. References

[1] http://www.superpower-inc.com/content/2g-hts-wire

[2] Goldacker W, Grilli F, Pardo E, Kario A, Schlachter SI and Vojenciak M 2014 *Supercond. Sci. Technol.* **27** 093001

[3] Van der Laan DC: 2015 Patent WO2015006350A3

[4] Shun Y *et al*., 2017 Patent CN107564623A

[5] Iwasa Y, Bascuñán J and Hahn S 2018 Patent US10079092B2

[6] Yagotintsev K, Anvar VA, Gao P, Dhalle MJ, Haugan TJ, van der Laan DC, Weiss JD, Hossain M S A and Nijhuis A 2020 *Supercond. Sci. Technol.* **33** 085009

[7] Breitschopf J, Chavez D, Elliott T, Kellams J, McIntyre P and Sattarov A 2020 *IOP Conf.*

Ser.: Mater. Sci. Eng. **756** 012031
[8] McIntyre P, Rogers J and Sattarov A 2021 *IEEE Trans. Appl. Superconduct.*, **31**, 5, 1-5, 10.1109
[9] Trillaud F, dos Santos G, Sotelo G 2021 *Materials*, **14**, 1892, 10.3390/ma14081892
[10] Choi S, Jo HC, Hwang YJ, Hahn S and Ko TK 2012 *IEEE Trans. Appl. Superconduct.* **2**, 3, 4904004
[11] Noguchi S 2019 *IEEE Trans. Appl. Supercond.* **29**, 5, 4602607
[12] Lu J, Goddard R, Han K and Hahn S 2017 *Physics: Instruments and Detectors* 1701.00447
[13] Martinez ACA, Ji Q, Prestemon SO, Wang X and Mary-Cuna GHI 2020 *IEEE Trans. Appl. Superconduct.* **30**, 4, 1-5, 6600605